frontiers | Frontiers in Energy Research

TYPE Original Research
PUBLISHED 20 December 2023
DOI 10.3389/fenrg.2023.1305076

Fuel-constrained joint heat and power dynamic economic environmental dispatch

Mousumi Basu[1], Chitralekha Jena[2], Baseem Khan[3,4]*, Ahmed Ali[4] and Pitshou Bokoro[4]

[1]Department of Power Engineering, Jadavpur University, Kolkata, India, [2]Department of Electrical Engineering, KIIT University, Bhubaneswar, India, [3]Department of Electrical and Computer Engineering, Hawassa University, Hawasa, Ethiopia, [4]Department of Electrical and Electronic Engineering Technology, University of Johannesburg, Johannesburg, South Africa

Check for updates

OPEN ACCESS

EDITED BY
Deepak Kumar,
Birla Institute of Technology, India

REVIEWED BY
Minh Quan Duong,
The University of Danang, Vietnam
Masoud Dashtdar,
Islamic Azad University, Iran

*CORRESPONDENCE
Baseem Khan,
baseem.khan04@gmail.com

RECEIVED 30 September 2023
ACCEPTED 01 December 2023
PUBLISHED 20 December 2023

CITATION
Basu M, Jena C, Khan B, Ali A and Bokoro P (2023), Fuel-constrained joint heat and power dynamic economic environmental dispatch.
Front. Energy Res. 11:1305076.
doi: 10.3389/fenrg.2023.1305076

The economical use of available fuel for producing electricity has been a very important challenge for power companies due to the continuously declining supply of fossil fuels. FCJHPDEED (fuel-constrained joint heat and power dynamic economic environmental dispatch) and JHPDEED (joint heat and power dynamic economic environmental dispatch) with DSM (demand-side management) integrating solar PV plants, WTGs (wind turbine generators), and PHS (pumped hydro storage) plants have been presented. Using SPEA 2 (strength Pareto evolutionary algorithm 2) and NSGA-II (non-dominated sorting genetic algorithm-II), FCJHPDEED and JHPDEED have been solved. It is seen that the results obtained without fuel constraints are more optimal than the results obtained with fuel constraints. The joint heat and power dynamic economic dispatch cost obtained with fuel constraints is approximately 2.14% more than the cost obtained without fuel constraints and joint heat and power dynamic emission dispatch, and the emission obtained with fuel constraints is approximately 6.7% more than the emission obtained without fuel constraints.

KEYWORDS

fuel-constrained co-generation units, fuel-constrained thermal generating units, demand-side management, dynamic economic environmental dispatch, optimization

1 Introduction

The primary source of electricity production until now has been fossil fuel-based power plants. There is a chance of a fuel shortage since fossil fuel production is progressively declining. Power producers are required to reorganize power production depending on the fuel that is available since fuel suppliers have added further restrictions to their fuel-providing agreement.

With the growing debate on climate alteration and pollution-free energy, wind power and solar power are increasingly utilized today as they are free from harmful emissions. However, renewable energy sources have their own challenges due to their irregularity and intermittent nature, which can cause fluctuations in power generation scheduling. This can be overcome by assimilating PHS plants to reduce power fluctuations.

The economic dispatch problem has been described briefly in Le et al. (2019); Dashtdar et al. (2022). Trefny and Lee have explained economic dispatch, taking into account fuel restrictions (Trefny and Lee, 1981). The fuel resource arrangement in managing power systems is described in Kumar and Vemuri (1984); Vemuri et al. (1984).

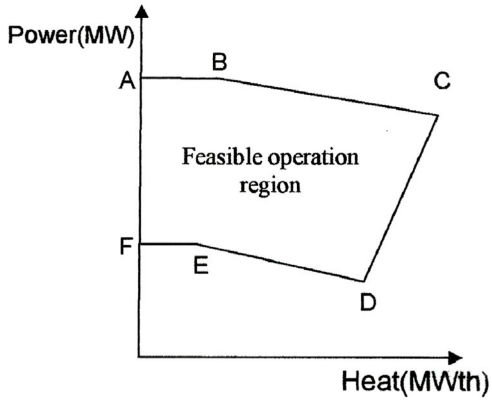

FIGURE 1
Heat-power viable workable area of a co-generation unit.

The optimal generation schedule of a small sovereign system using WTGs and solar PV facilities, both of which produce no pollution, has been described in Bakirtzis and Gavanidou (1992). However, due to their limited generation capacity, the combined use of different energy-producing systems (Mondal et al., 2013; Khan et al., 2015) is increasing rapidly.

PHS plants are drawing a lot of interest throughout the world (Perez-Diaz and Jim, 2016) because of their capacity to store energy. The main purpose of a PHS plant is to pump water from the lower reservoir into the higher reservoir in order to save low-cost extra electric energy generated in off-peak power demand times (Wood and Wollenberg, 1984; Fadil and Urazel, 2013). This hoarded energy is used to generate energy throughout peak power demand periods.

Electricity is produced inefficiently using fossil fuels. Heat is the main kind of energy destroyed during the conversion process. Co-generation utilizes this heat efficiently and produces lower harmful gas emanation. Utilizing CHPDED, the production of electricity and heat is distributed in a way that minimizes the overall cost while also meeting a number of limitations. Several methods (Rooijers and van Amerongen, 1994; Guo et al., 1996; Su and Chiang, 2004; Vasebi et al., 2007; Wang and Singh, 2008; Subbaraj et al., 2009; Mohammadi-Ivatloo et al., 2013; Basu, 2016) have been described to resolve this problem.

JHPDEED optimizes the total generation cost and emission level of steam turbine generators, co-generation units, and heat-only units throughout a particular period of time, considering power ramp rate limitations of co-generation and steam turbine generating units.

Several approaches to resolve economic dispatch, assimilating WTGs and solar PV plants, are explained in Hetzer et al. (2008); Reddy et al. (2015); Tang et al. (2015); Li et al. (2016); Liu and Nair (2016); Peng et al. (2016); Yang et al. (2016); Liu et al. (2017).

According to the International Energy Agency's strategy plan, DSM has been established as the most significant choice of the overall energy policy directives. DSM can reduce the price and boost system safety (Yousefi et al., 2013).

Here, both FCJHPDEED and JHPDEED with DSM have been described. The system comprises thermal generators, heat-only units, co-generation units, solar PV plants, WTGs, and PHS plants. The uncertainty of WTGs and solar PV plants has been considered. The primary restrictions are restrictions on different fuel types for co-generation units and thermal generators, PHS plants, time-varying load demand, and on the generation capabilities and power ramp rates. The valve-point effect and forbidden viable region of steam turbine generating units have been considered. Both FCJHPDEED and JHPDEED with DSM have been solved using SPEA 2 and NSGA-II.

2 Formulation of the problem

Here, the system considered has fuel-constrained steam turbine generating units, heat-only units, co-generation units, WTGs, PHS plants, and solar PV plants. Figure 1 demonstrates the heat-power possible range of a combined cycle co-generation unit. Power output and heat output are indivisible. Heat-power workable county is enfolded by the frontier ABCDEF.

The output power of the steam turbine generating units, WTGs, solar PV plants, and PHS plants and the heat output of heat-only units are limited by the individual minimum and maximum limits. Power is generated by steam turbine generating units, WTGs, solar PV plants, co-generation units, and PHS plants, while heat is generated by heat-only units and co-generation units.

The FCJHPDEED issue with DSM-integrating solar PV plants, WTGs, and PHS plants distributes heat and power generation among all dedicated thermal generating units, WTGs, co-generation units, PHS plants, solar PV plants, and heat-only units in a way that the emission and total price are optimized over a specific time period while satisfying a number of constraints, including generation limit restrictions, power and heat balance constraints, and dissimilar types of fuel construction. When formulating the FCJHPDEED issue, the objective functions and restrictions mentioned below are considered.

2.1 Objectives

2.1.1 Cost

The total price is expressed as

$$F_C = \sum_{t=1}^{T}\Bigg[\sum_{i=1}^{N_s} f_{sit}(P_{sit}) + \sum_{i=1}^{N_c} f_{cit}(P_{cit}, H_{cit}) + \sum_{i=1}^{N_h} f_{hit}(H_{hit}) + \sum_{i=1}^{N_W}\{Kd_{wi}\times P_{wit} + Oe_{wit}(P_{wit}) + Ue_{wit}(P_{wit})\} + \sum_{i=1}^{N_{PV}}\{Kd_{si}\times P_{PVit} + Oe_{PVit}(P_{PVit}) + Ue_{PVit}(P_{PVit})\}\Bigg]. \quad (1)$$

The fuel price function of the ith thermal generator at hour t, considering the valve-point effect (Walters and Sheble, 1993), can be expressed as

$$f_{sit}(P_{sit}) = a_{si} + b_{si}P_{sit} + c_{si}P_{sit}^2 + \left|d_{si}\times \sin\{e_{si}\times (P_{si}^{\min} - P_{sit})\}\right|. \quad (2)$$

The price function of the ith co-generation unit (Vemuri et al., 1984) at hour t can be shown as

$$f_{cit}(\mathrm{P}_{cit},\mathrm{H}_{cit})=\alpha_{ci}+\beta_{ci}\mathrm{P}_{cit}+\gamma_{ci}\mathrm{P}_{cit}^2+\delta_{ci}\mathrm{H}_{cit}+\varepsilon_{ci}\mathrm{H}_{cit}^2+\xi_{ci}\mathrm{P}_{cit}\mathrm{H}_{cit}]. \quad (3)$$

The price function of the ith heat-only unit at time t can be shown as

$$f_{hit}(\mathrm{H}_{hit})=\varphi_{hi}+\psi_{hi}\mathrm{H}_{hit}+\chi_{hi}\mathrm{H}_{hit}^2. \quad (4)$$

The reserve and penalty price of wind power (Hetzer et al., 2008) can be shown as

$$Oe_{wit}(\mathrm{P}_{wit})=oe_{wi}\times\int_{\mathrm{P}_{wit}^{\min}}^{\mathrm{P}_{wit}}(\mathrm{P}_{wit}-y)\times f_w(y)dy. \quad (5)$$

$$Ue_{wit}(\mathrm{P}_{wit})=ue_{wi}\times\int_{\mathrm{P}_{wit}}^{\mathrm{P}_{wit}^{\max}}(y-\mathrm{P}_{wit})\times f_w(y)dy. \quad (6)$$

The reserve and penalty price of solar power (Liang and Liao, 2007) can be shown as

$$Oe_{PVit}(\mathrm{P}_{PVit})=oe_{PVi}\times\int_{\mathrm{P}_{PVit}^{\min}}^{\mathrm{P}_{PVit}}(\mathrm{P}_{PVit}-x)\times f_{PV}(x)dx. \quad (7)$$

$$Ue_{PVit}(\mathrm{P}_{PVit})=ue_{PVi}\times\int_{\mathrm{P}_{PVit}}^{\mathrm{P}_{PVit}^{\max}}(x-\mathrm{P}_{PVit})\times f_{PV}(x)dx. \quad (8)$$

2.1.2 Emission

Thermal power plants are the main sources of sulfur oxides, nitrogen oxides, and carbon dioxide. Emission from a steam turbine generating unit is the addition of quadratic function and exponential function (Gent and Lamont, 1971). The total emission from steam turbine generating units, co-generation units, and heat-only units can be expressed as

$$\mathrm{E_T}=\sum_{t=1}^{\mathrm{T}}\left[\sum_{i=1}^{\mathrm{N}_s}\left\{\mu_{si}+\kappa_{si}\mathrm{P}_{sit}+\pi_{si}\mathrm{P}_{sit}^2+\sigma_{so}e^{(\theta_{si}\mathrm{P}_{sit})}\right\}+\sum_{i=1}^{\mathrm{N}_c}\tau_{ci}\mathrm{P}_{cit}+\sum_{i=1}^{\mathrm{N}_h}\upsilon_{hi}\mathrm{H}_{hit}\right]. \quad (9)$$

2.2 Constraints

i)Power balance constraints:

$$\sum_{i=1}^{\mathrm{N}_s}\mathrm{P}_{sit}+\sum_{i=1}^{\mathrm{N}_c}\mathrm{P}_{cit}+\sum_{i=1}^{\mathrm{N}_w}\mathrm{P}_{wit}+\sum_{i=1}^{\mathrm{N}_{PV}}\mathrm{P}_{PVit}+\sum_{i=1}^{\mathrm{N}_{pump}}\mathrm{P}s_{ghit}=(1-DR_t)\times LF_{Base,t}+Ls_t+\mathrm{P}_{Lt},\ t\in\mathrm{T}_{gen}, \quad (10)$$

$$\sum_{i=1}^{\mathrm{N}_s}\mathrm{P}_{sit}+\sum_{i=1}^{\mathrm{N}_c}\mathrm{P}_{cit}+\sum_{i=1}^{\mathrm{N}_w}\mathrm{P}_{wit}+\sum_{i=1}^{\mathrm{N}_{PV}}\mathrm{P}_{PVit}-\sum_{i=1}^{\mathrm{N}_{pump}}\mathrm{P}s_{phit}=(1-DR_t)\times LF_{Base,t}+Ls_t+\mathrm{P}_{Lt},\ t\in\mathrm{T}_{pump}, \quad (11)$$

$$\sum_{i=1}^{\mathrm{N}_s}\mathrm{P}_{sit}+\sum_{i=1}^{\mathrm{N}_c}\mathrm{P}_{cit}+\sum_{i=1}^{\mathrm{N}_w}\mathrm{P}_{wit}+\sum_{i=1}^{\mathrm{N}_{PV}}\mathrm{P}_{PVit}=(1-DR_t)\times LF_{Base,t}+Ls_t+\mathrm{P}_{Lt},\ t\in\mathrm{T}_{change\_over}. \quad (12)$$

Whilst power demand is cut back because of DRP, $Ls_t = 0$ during that time. Similar to how it is transferred to the basic power demand, the demand for electricity does not decrease at that time.

Loss in transmission P_{Lt} is affirmed as

$$\mathrm{P}_{Lt}=\sum_{i=1}^{\mathrm{N_T}}\sum_{j=1}^{\mathrm{N_T}}\mathrm{P}_{it}B_{ij}\mathrm{P}_{jt}+\sum_{i=1}^{\mathrm{N_T}}B_{0i}\mathrm{P}_{it}+B_{00}. \quad (13)$$

The number of plants $\mathrm{N_T}=\mathrm{N}_s+\mathrm{N}_c+\mathrm{N}_w+\mathrm{N}_{PV}$, and P_{it} is the respective steam turbine, co-generation, wind turbine, and solar PV generation.

ii) Fuel delivery constraints:

Over the course of the scheduling horizon, the total fuel provided to all co-generation units and steam turbine generating units should match the fuel that is supplied by the purveyor.

$$\sum_{i=1}^{\mathrm{N}_s}Fst_{im}+\sum_{i=1}^{\mathrm{N}_c}Fsc_{im}-F_{Dm}=0,\ m\in\mathrm{M}. \quad (14)$$

iii) Fuel storage constraints of steam turbine generators:

The residual fuel at the start of the subsequent interlude is calculated by subtracting the fuel burned at the thermal generator from the fuel volume of every steam turbine generating unit at the start of every interlude plus the fuel provided to that steam turbine generating unit.

$$Vst_{im}=Vst_{i(m-1)}+Fst_{im}-\sum_{t=1}^{t_m}\left[\eta_{si}+\delta_{si}\mathrm{P}_{sit}+\mu_{si}\mathrm{P}_{sit}^2+\left|\lambda_{si}\sin\{\rho_{si}(\mathrm{P}_{si}^{\min}-\mathrm{P}_{sit})\}\right|\right],\ i\in\mathrm{N}_s,\ m\in\mathrm{M}. \quad (15)$$

iv) Fuel delivery limits of steam turbine generators:

Fuel that is delivered to each steam turbine generating unit at every interlude must be within its lower limit $Fst^{\min}$ and upper limit $Fst^{\max}$.

$$Fst_i^{\min}\le Fst_{im}\le Fst_i^{\max},\ i\in\mathrm{N}_s,\ m\in\mathrm{M}. \quad (16)$$

v) Fuel storage limits of steam turbine generators:

The fuel storage limit of each steam turbine generating unit at each interlude must be within its lower limit $Vst^{\min}$ and upper limit $Vst^{\max}$.

$$Vst_i^{\min}\le Vst_{im}\le Vst_i^{\max},\ i\in\mathrm{N}_s,\ m\in\mathrm{M}. \quad (17)$$

vi) Fuel storage constraints of co-generation units:

The amount of fuel available at the start of the subsequent interlude is determined by the fuel volume of each co-generation unit at the beginning of each interlude, fuel supplied to that co-generation unit, and fuel burned at that co-generation unit.

$$Vsc_{im}=Vsc_{i(m-1)}+Fsc_{im}-\sum_{t=1}^{t_m}[\alpha_{si}+\beta_{si}\mathrm{P}_{cit}+\gamma_{si}\mathrm{P}_{cit}^2+\delta_{si}\mathrm{H}_{cit}+\varepsilon_{si}\mathrm{H}_{cit}^2+\xi_{si}\mathrm{P}_{cit}\mathrm{H}_{cit}],\ i\in\mathrm{N}_s,\ m\in\mathrm{M}. \quad (18)$$

vii) Fuel delivery limits of co-generation units:

Fuel delivered to each co-generation unit at each interlude must be within its minimum limit Fsc^{min} and maximum limit Fsc^{max}.

$$Fsc_i^{min} \le Fsc_{im} \le Fsc_i^{max},\ i \in N_s,\ m \in M. \tag{19}$$

viii) Fuel storage limits of co-generation units:

The fuel storage limit of each co-generation unit at each interlude must be within its minimum limit Vsc^{min} and maximum limit Vsc^{max}.

$$Vsc_i^{min} \le Vsc_{im} \le Vsc_i^{max},\ i \in N_s,\ m \in M. \tag{20}$$

ix) Generation limits of the thermal generator:

$$P_{si}^{min} \le P_{sit} \le P_{si}^{max}\ i \in N_s,\ t \in T. \tag{21}$$

x) Forbidden workable region of thermal generating units:

The restricted area of a steam turbine generating unit is due to the shaft bearing tremor caused by a steam valve or a flaw in the machine or supporting equipment. It is challenging to determine the input–output curve's shape in the hinterland of a possible but restricted zone using actual routine testing. In actuality, avoiding operating in certain areas results in the biggest cost-saving strategy. The following is a possible area of operation for the i th steam turbine generator at this time t:

$$\begin{aligned} &P_{si}^{min} \le P_{sit} \le P_{si,1}^{l},\\ &P_{si,j-1}^{u} \le P_{sit} \le P_{si,j}^{l}\ ;\ j = 2, 3, ..., n_i,\\ &P_{si,n_{ij}}^{u} \le P_{sit} \le P_{si}^{max}, \end{aligned} \tag{22}$$

where j indicates the number of proscribed workable county. $P_{si,j-1}^{u}$ is the maximum limit of the $(j-1)$th forbidden workable region of the ith generator. The minimum limit of the jth forbidden region of the ith generating unit is $P_{si,j}^{l}$. The number of forbidden workable regions of the ith generating unit is n_i.

xi) Power ramp rate limit constraints of steam turbine generators and co-generation units:

$$P_{sit} - P_{si(t-1)} \le UR_{si},\ i \in N_s,\ t \in T, \tag{23}$$

$$P_{si(t-1)} - P_{sit} \le DR_{si},\ i \in N_s,\ t \in T, \tag{24}$$

$$P_{cit} - P_{ci(t-1)} \le UR_{ci},\ i \in N_c,\ t \in T, \tag{25}$$

$$P_{ci(t-1)} - P_{cit} \le DR_{ci},\ i \in N_c,\ t \in T. \tag{26}$$

xii) Heat balance constraints:

$$\sum_{i=1}^{N_c} H_{cit} + \sum_{i=1}^{N_h} H_{hit} = H_{Dt},\ t \in T. \tag{27}$$

xiii) Capacity boundary limits of co-generation units:

The heat output and power output of the co-generation unit are inseparable, and they intrude one another. $P_c^{min}(H_c)$, $P_c^{max}(H_c)$, $H_c^{min}(P_c)$, and $H_c^{max}(P_c)$ are linear inequalities which depict the feasible area of the co-generation unit.

$$P_{ci}^{min}(H_{ci}) \le P_{cit} \le P_{ci}^{max}(H_{ci}),\ i \in N_c \text{ and } t \in T, \tag{28}$$

$$H_{ci}^{min}(P_{ci}) \le H_{cit} \le H_{ci}^{max}(P_{ci}),\ i \in N_c \text{ and } t \in T. \tag{29}$$

xiv) Capability boundary limits of heat-only units:

$$H_{hi}^{min} \le H_{hit} \le H_{hi}^{max},\ i \in N_h \text{ and } t \in T. \tag{30}$$

xv) Wind power model:

The WTG's output power mostly depends on wind velocity. Cut-in pace, rated pace, and cut-out pace of wind are used to clarify the nonlinear connection between wind velocity and output power. Power output (Giorsetto and Utsurogi, 1983) of the ith WTG at hour t for a specific wind velocity can be signified as

$$\begin{aligned} P_{wit} &= 0,\ \text{for } vw_t < vc_{in} \text{ and } vw_t > vc_{out},\\ P_{wit} &= \left(A_w + B_w vw_t + C_w vw_t^2\right)P_{wri},\ \text{for } vc_{in} \le vw_t < vw_r,\\ P_{wit} &= P_{wri},\ \text{for } vw_r \le vw_t \le vc_{out}. \end{aligned} \tag{31}$$

Constants A_w, B_w, and C_w are functions of vw_r and vc_{in} and are computed utilizing the following equations:

$$A_w = \frac{1}{(vc_{in} - vw_r)^2}\left[vc_{in}(vc_{in} + vw_r) - 4vc_{in}vw_r\frac{(vc_{in} - vw_r)^3}{2vw_r}\right]. \tag{32}$$

$$B_w = \frac{1}{(vc_{in} - vw_r)^2}\left[2 - 4\frac{\left(\frac{4}{vc_{in}} + vw_r\right)^3}{2vw_r}\right]. \tag{33}$$

$$C_w = \frac{1}{(vc_{in} - vw_r)^2}\left[4(vc_{in} + vw_r) + \frac{(vc_{in} + vw_r)^3 - (3vc_{in} + vw_r)}{2vw_r}\right]. \tag{34}$$

xvi) Solar power model:

The power output (Shilaja and Ravi, 2017) acquired from the ith solar PV power plant at hour t is signified as

$$P_{PVit} = P_{PVri} \times \left[1 + \alpha_r \times \left(T_{ref} - T_{ambt}\right)\right] \times \frac{G_r}{1000}. \tag{35}$$

xvii) Pumped hydro storage plant constraints:

Whilst the PHS unit runs in the generating type and decides to run in the pumping type or *vice versa*, the PHS unit must be switched off for at least 1 hour because of physical restrictions of the unit, and it is recognized as switching time.

$$V_{res,l(t+1)} = V_{res,lt} + Q_{phlt}\left(Ps_{phlt}\right),\ l \in N_{pump},\ t \in T_{pump}, \tag{36}$$

$$V_{res,l(t+1)} = V_{res,lt} - Q_{ghlt}\left(Ps_{ghlt}\right),\ l \in N_{pump},\ t \in T_{gen}, \tag{37}$$

$$V_{res,l}^{(t+1)} = V_{res,l}^{t},\ l \in N_{pump} \text{ and } t \in T_{change_{over}}, \tag{38}$$

$$P_{ghl}^{min} \le Ps_{ghlt} \le P_{ghl}^{max}\ l \in N_{pump},\ t \in T_{gen}, \tag{39}$$

$$P_{phl}^{min} \le Ps_{phlt} \le P_{phl}^{max}\ l \in N_{pump},\ t \in T_{pump}, \tag{40}$$

$$V_{res,l}^{min} \le V_{res,lt} \le V_{res,l}^{max},\ l \in N_{pump},\ t \in T. \tag{41}$$

The starting and ending volumes of the water of the upper reservoir of the PHS plant are presumed to be identical here.

$$V_{res,l0} = V_{res,lT} = V^{start}_{res,l} = V^{end}_{res,l}. \quad (42)$$

Demand-side management (DSM)

DSM initiates many benefits (Yousefi et al., 2013). DSM is categorized as DRP (demand response program), planned conservation, and so on. In this manuscript, DRP is utilized, and it is shaped as the TOU (time-of-use) program (Mehdizadeh and Taghizadegan, 2017). In the TOU program, a small proportion of demand is switched from peak to off-peak hours while keeping the overall demand constant. Equation 43 explains the TOU program, while Eq. 44 restricts it (47).

$$L_t = (1 - DR_t) \times LF_{Base} + Ls_t, \quad (43)$$

$$\sum_{t=1}^{T} L_{st} = \sum_{t=1}^{T} DR_t \times LF_{Base,t}, \quad (44)$$

$$L_{Incl_t} = Incl_t \times LF_{Base,t}, \quad (45)$$

$$DR_t \le DR^{\max}, t \in T, \quad (46)$$

$$Incl_t \le Incl^{\max}, t \in T \forall t = 1: 24. \quad (47)$$

3 Principle of multi-objective optimization

Most actual-world issues require concurrent optimization of various conflicting objective functions. MOO with contradictory objective functions generates a number of optimum solutions in place of one optimum solution as no solution is superior to every other relating to all objective functions. Francis Ysidro Edgeworth proposed the concept of a trade-off optimality criterion in 1881, and Vilfredo Pareto clarified it in 1896. It is usually referred to as Pareto optimum, and optimum solutions are referred to as Pareto-optimal solutions.

The following is affirmed for a MOO problem with several goals and equality and inequality constraints:

$$\text{Minimize } f_i(x), i = 1, \ldots, N_{obj} \quad (48)$$

subject to

$$\begin{cases} g_k(x) = 0 & k = 1, \ldots, K \\ h_l(x) \le 0 & l = 1, \ldots, L, \end{cases} \quad (49)$$

where f_i is denoted as the ith objective function, x is denoted as the decision vector that symbolizes a solution, and N_{obj} is denoted as the number of objectives. Decision vector x_1 dominates the decision vector x_2 if both the conditions mentioned in (50) and (51) are attained.

a. **Sufficient condition:** The decision vector x_1 is better than x_2 for all the objectives.

$$\forall i \in \{1, \ldots, N_{obj}\}, f_i(x_1) \le f_i(x_2). \quad (50)$$

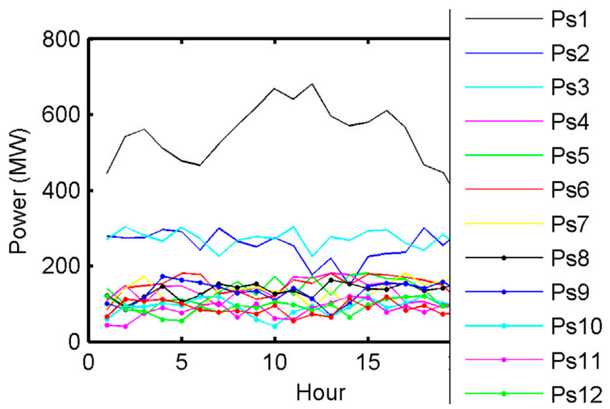

FIGURE 2
Output power of thermal generators from FCJHPDEED using NSGA-II.

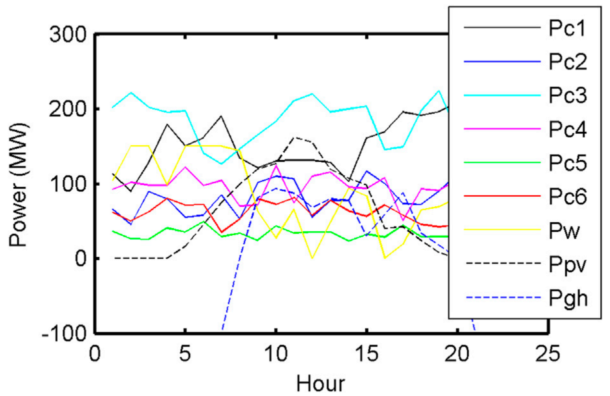

FIGURE 3
Output power of co-generation units, WTG, solar PV plant, and PHS plant from FCJHPDEED using NSGA-II.

b. **Necessary condition:** The decision vector x_1 is firmly superior to the decision vector x_2 as a minimum one of the objective functions.

$$\exists i \in \{1, \ldots, N_{obj}\}, f_i(x_1) < f_i(x_2). \quad (51)$$

4 Non-dominated sorting genetic algorithm-II

Srinivas and Deb (1994) ascertained NSGA for competing with MOO problems. Non-domination has been exploited as a grading decisive factor of solutions, and on the other hand, fitness distribution has been exploited for diversification control in the investigated space. Since NSGA is very receptive to fitness distribution parameters, Deb et al. (2002) initiated NSGA-II, which generates more consistent solutions swifter than its ancestor.

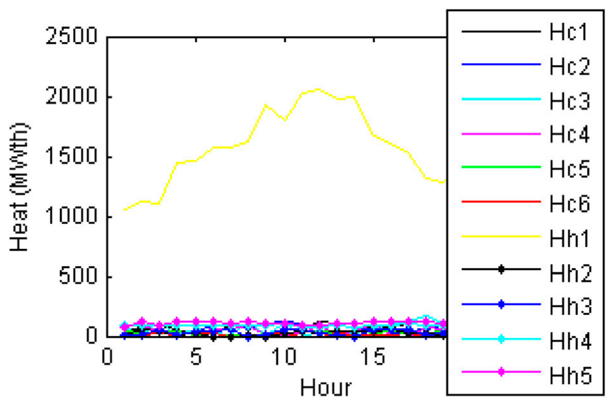

FIGURE 4
Heat output of co-generation units and heat-only units from FCJHPDEED using NSGA-II.

TABLE 1 Fuel delivered (ton) to thermal generating units acquired from FCJHPDEED using NSGA-II.

Interval	1	2	3	4	5	6
Fs_1	1,582.6	4,986.0	2,684.1	3,045.0	3,494.7	165.1
Fs_2	2,171.3	1,029.0	1,528.2	1,230.1	1,658.9	838.6
Fs_3	131.1	793.6	1,444.7	2,435.6	213.6	2,295.2
Fs_4	722.8	1,369.4	1496.9	1,294.3	1,446.0	1,482.2
Fs_5	1,421.0	64.7	608.5	625.4	1,480.4	630.0
Fs_6	1,419.9	9.3	1,220.8	1,214.4	804.3	248.2
Fs_7	1,257.5	166.2	311.8	1,279.5	1,272.2	1,028.4
Fs_8	1,011.6	502.6	1,500.0	623.7	1,163.4	674.9
Fs_9	1,500.0	1,335.8	1,005.3	1,146.8	498.1	1,336.9
Fs_{10}	240.6	888.8	595.6	530.5	142.3	856.8
Fs_{11}	287.4	565.9	214.1	597.6	46.3	781.9
Fs_{12}	553.0	680.6	504.4	609.8	716.4	609.3
Fs_{13}	668.6	722.6	634.2	604.1	492.5	854.6

5 Strength Pareto evolutionary algorithm 2

Strength Pareto evolutionary algorithm 2 (SPEA 2) (Zitzler et al., 2001) is the superior edition of SPEA. It blends a well-tuned fitness assignment approach, a density assessment technique, and an improved archive truncation technique with the conventional SPEA. In SPEA 2, the fitness value assigned to every entity is computed based on the strength value and the density degree. As each individual has its own value of density, the calculation starts with sorting the values of all objectives. The density value of every entity is the same as the sum of the difference between each objective value and its nearest neighbor. The fitness value is the summation of the strength value and the density degree. SPEA 2 uses an improved archive truncation method, where the size of the external storage file is fixed. The crossover and mutation procedure only occur in the storage file.

TABLE 2 Fuel delivered (ton) to co-generation units acquired from FCJHPDEED using NSGA-II.

Interval	1	2	3	4	5	6
Fsc_1	1,786.4	2,258.7	1,350.6	2,456.2	1,305.4	1,780.9
Fsc_2	479.3	16.0	990.0	233.1	887.0	1,230.1
Fsc_3	1,435.6	1,899.0	2,443.5	2,276.3	2,196.6	2,467.8
Fsc_4	759.9	421.0	1,329.7	573.1	1,477.5	1,013.5
Fsc_5	370.4	390.6	237.5	324.2	102.2	96.0
Fsc_6	200.9	900.0	900.0	900.0	602.2	609.6

6 Numerical results

NSGA-II and SPEA 2 have been utilized for solving FCJHPDEED and JHPDEED with DSM integrating WTGs, PHS plants, and solar PV plants.

Total price and emission are two conflicting objective functions. To elucidate contrary relationships among objective functions, each objective function, namely, total price and total emission, is lowered distinctly by using RCGA (real-coded genetic algorithm). The population size, maximum number of iterations, crossover, and mutation probabilities are chosen as 100, 300, 0.9, and 0.2, respectively.

SPEA 2 and NSGA-II are used for optimizing total price and total emission objectives concurrently. The population size, maximum number of iterations, crossover, and mutation probabilities are taken as 20, 30, 0.2, and 0.9 for SPEA 2 and NSGA-II, respectively.

An equivalent WTG, an equivalent solar PV plant, an equivalent PHS plant, 13 thermal generating units with a banned working region and valve point impact, six co-generation units, and five heat-only units are all included in the test system. The data on co-generation units, steam turbine generating units, heat-only units, and hourly heat and power demand have been taken from Basu (2019). The whole schedule is divided into six 4-h intermissions, totaling 1 day. Table A contains information on coal-burning thermal generating units, including emission coefficients, coal "consumption coefficients, fuel delivery and storage limits, and starting fuel storage. 1. Table A contains information on the co-generation unit, including coal consumption coefficients, fuel supply and storage limits, and starting fuel storage. 2. Table A lists the emission coefficients for heat-only and co-generation units. 3. Table A lists the fuel that was supplied throughout the scheduled period.

The WTG rating is denoted as P_{wr} = 150 MW. The direct cost coefficient for WTG is chosen as Kd_w= 7. Penalty and reserve cost coefficients for WTG are chosen as ue_w= 1 and oe_w= 2, respectively. Cut-in, cut-out, and rated wind paces are v_{in}= 5 m/s, v_o= 25 m/s and v_r= 15 m/s, respectively.

The solar PV plant rating is denoted as P_{sr} = 175 MW. The direct cost coefficient (Kd_s) for the solar PV plant is selected as 6. The penalty and reserve cost coefficients for the solar PV plant are selected as ue_{PV}= 1 and oe_{PV}= 2, respectively. Solar radiation in the standard environment (G_{std}) and a certain radiation point (R_c) have been chosen as 1000 W/m^2 and 150 W/m^2, respectively. Solar

TABLE 3 Comparison of performance.

		Cost ($)	Emission (kg)
Joint heat and power dynamic economic dispatch	With fuel constraints	3,402,717	3,249
	Without fuel constraints	3,329,926	3,318
Joint heat and power dynamic environmental dispatch	With fuel constraints	3,809,199	2,568
	Without fuel constraints	3,851,192	2,396
FCJHPDEED	NSGA-II	3,614,163	2,851
	SPEA 2	3,631,141	2,876
JHPDEED	NSGA-II	3,595,131	2,863
	SPEA 2	3,607,718	2,840

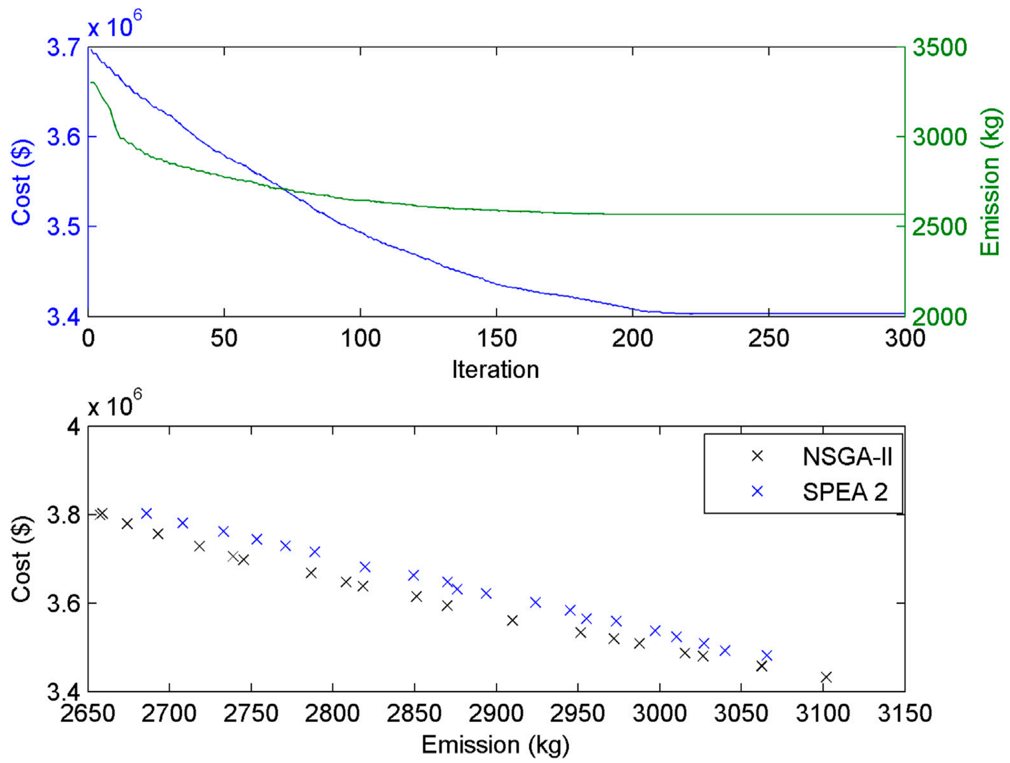

FIGURE 5
Cost convergence, emission convergence, and Pareto-optimal front obtained from the last iteration with fuel constraints.

irradiation and wind velocity's maximum and minimum predicted limits are obtained from Walters and Sheble (1993). The reference temperature (T_{ref}) and temperature coefficient (α_r) are chosen as 25^oC and $-0.25\%/k$ (per Kelvin), respectively. The PHS plant has subsequent features:

Generating mode:

Q_{ght} is positive, P_{ght} is positive, $0 \le P_{ght} \le 100$ MW, and $Q_{ght}(P_{ght}) = 70 + 2P_{ght}$ acre-ft/hr

Pumping mode:

Q_{pht} is negative, P_{pht} is negative, $-100MW < P_{pht} \le 0MW$, $Q_{pht}(P_{pht}) = -200$ acre-ft/h, and $P_{pht} = -100$ MW

Working restrictions: The PHS plant is allowed to operate only at −100 MW while pumping. The reservoir begins at 3000 acre/ft and should be at 3000 acre/ft at the ending of 24 h.

The 12, 13, and 14 hours are peak power demand hours. It is observed that 10% of 12-, 13-, and 14-hour power demands is transferred to the second, third, and fourth hour throughout DSM, respectively.

Power generation of thermal generating units, solar PV plants, WTGs, co-generation units, and PHS plants obtained from FCJHPDEED utilizing NSGA-II is portrayed in Figure 2 and Figure 3. Heat generation of heat-only units and co-generation units obtained from FCJHPDEED utilizing NSGA-II is portrayed in Figure 4.

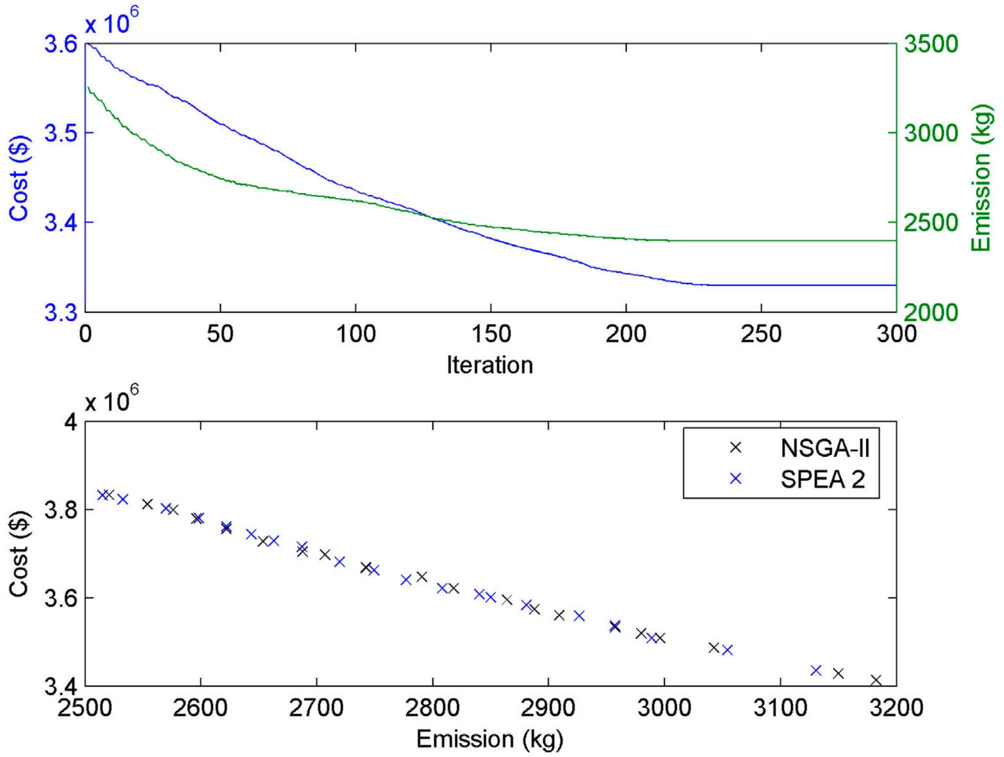

FIGURE 6
Cost convergence, emission convergence, and Pareto-optimal front obtained from the last iteration without fuel constraints.

Fuel delivered to thermal generators and co-generation units obtained from FCJHPDEED using NSGA-II is mentioned in Table 1 and Table 2. TC and total emission acquired from CHPDED and joint heat and power dynamic environmental dispatch with and without fuel constraints are summarized in Table 3. Figure 5 and Figure 6 portray cost convergence characteristics, emission convergence characteristics, and the Pareto-optimal front obtained from the last iteration using SPEA 2 and NSGA-II with and without fuel constraints, respectively.

Because of space limitations, detailed results obtained from joint heat and power dynamic economic dispatch, CHPDED with and without fuel constraints, JHPDEED without fuel constraints, and FCJHPDEED with fuel constraints using SPEA 2 cannot be given here.

7 Conclusion

In the present work, NSGA-II and SPEA 2 are used in order to solve real-world fuel-constrained joint heat and power dynamic economic environmental dispatch (FCJHPDEED) and joint heat and power dynamic economic environmental dispatch (JHPDEED) with DSM integrating the WTG, solar PV plant, and PHS plant. It is seen from numerical results that fuel consumption is satisfactorily managed for satisfying constraints inflicted by fuel purveyors utilizing the proposed techniques. It is observed that the results obtained without fuel constraints are more optimal than the results obtained with fuel constraints. In the case of joint heat and power dynamic economic emission dispatch, the cost acquired with fuel constraints is approximately 0.53% more than the cost acquired without fuel constraints, and the emission acquired with fuel constraints is approximately 0.42% lower than the emission acquired without fuel constraints. Although optimal dispatch is not achieved at all times, however, this is typically much better than the penalty imposed due to fuel constraint violations.

Data availability statement

The original contributions presented in the study are included in the article/Supplementary Material; further inquiries can be directed to the corresponding author.

Author contributions

MB: conceptualization, data curation, formal analysis, investigation, methodology, project administration, resources, software, supervision, validation, visualization, writing–original draft, and writing–review and editing. CJ: conceptualization, data curation, formal analysis, investigation, methodology, project administration, resources, software, supervision, validation, visualization, and writing–review and editing. BK: conceptualization, data curation, formal analysis, methodology, project administration, resources, software, supervision, validation, visualization, writing–original draft, and writing–review and editing. AA: conceptualization, data curation, formal analysis, investigation, methodology, project administration, resources, software, supervision, validation, visualization, and writing–review and editing. PB: data curation, formal analysis, methodology, project

administration, resources, software, supervision, validation, visualization, and writing–review and editing.

Funding

The author(s) declare that no financial support was received for the research, authorship, and/or publication of this article.

Conflict of interest

The authors declare that the research was conducted in the absence of any commercial or financial relationships that could be construed as a potential conflict of interest.

Publisher's note

Supplementary material

The Supplementary Material for this article can be found online at: https://www.frontiersin.org/articles/10.3389/fenrg.2023.1305076/full#supplementary-material

References

Bakirtzis, A. G., and Gavanidou, E. S. (1992). Optimum operation of a small autonomous system with unconventional energy sources. *Electr. Power Syst. Res.* 23 (1), 93–102. doi:10.1016/0378-7796(92)90056-7

Basu, M. (2019). Combined Heat and Power Dynamic Economic Dispatch with demand side management incorporating renewable energy sources and pumped hydro energy storage. *IET Gener. Transm. Distrib.* 13 (17), 3771–3781. doi:10.1049/iet-gtd.2019.0216

Basu, M. (2016). Group search optimization for combined heat and power economic dispatch. *Int. J. Electr. Power and Energy Syst.* 78, 138–147. doi:10.1016/j.ijepes.2015.11.069

Dashtdar, M., Flah, A., Mohammad Sadegh, S., Hosseinimoghadam, Rami Reddy, Ch., Kotb, H., et al. (2022). Solving the environmental/economic dispatch problem using the hybrid FA-GA multi-objective algorithm. *Energy Rep.* 8, 13766–13779. doi:10.1016/j.egyr.2022.10.054

Deb, K., Pratap, A., Agarwal, S., and Meyarivan, T. (2002). A fast and elitist multiobjective genetic algorithm: NSGA-II. *IEEE Trans. Evol. Comput.* 6 (2), 182–197. doi:10.1109/4235.996017

Fadil, S., and Urazel, B. (2013). Solution to security constrained non-convex pumped-storage hydraulic unit scheduling problem by modified sub-gradient algorithm based on feasible values and pseudo water price. *Electr. Power Components Syst.* 41, 111–135. doi:10.1080/15325008.2012.732660

Gent, M. R., and Lamont, J. W. (1971). Minimum emission dispatch. *IEEE Trans. PAS* (90), 2650–2660. doi:10.1109/tpas.1971.292918

Giorsetto, P., and Utsurogi, K. F. (1983). Development of a new procedure for reliability modeling of wind turbine generators. *IEEE Trans. Power App. Syst.* 102 (1), 134–143. doi:10.1109/tpas.1983.318006

Guo, T., Henwood, M. I., and Ooijen, M. V. (1996). An algorithm for combined heat and power economic dispatch. *IEEE Trans. Power Syst.* 11 (4), 1778–1784. doi:10.1109/59.544642

Hetzer, J., Yu, D. C., and Bhattarai, K. (2008). An economic dispatch model incorporating wind power. *IEEE Trans. Energy Convers.* 23 (2), 603–611. doi:10.1109/tec.2008.914171

Khan, N. A., Awan, A. B., Mahmood, A., Sohail, R., Zafar, A., and Sidhu, G. A. S. (2015). Combined emission economic dispatch of power system including solar photo voltaic generation. *Energy Convers. Manag.* 92 (1), 82–91. doi:10.1016/j.enconman.2014.12.029

Kumar, A. B. R., and Vemuri, S. (1984). Fuel resource scheduling, Part-II-contrained economic dispatch. *IEEE Trans. Power Apparatus Syst.* 7, 1549–1555. PAS-103. doi:10.1109/TPAS.1984.318624

Le, C., Trung Nguyen, T., Trong Hien, C., and Quan Duong, M. (2019). A novel social spider optimization algorithm for large-scale economic load dispatch problem. *Energies* 12 (6), 1075. doi:10.3390/en12061075

Li, Y. Z., Wu, Q. H., Jiang, L., Yang, J. B., and Xu, D. L. (2016). Optimal power system dispatch with wind power integrated using nonlinear interval optimization and evidential reasoning approach. *IEEE Trans. Power Syst.* 31 (3), 2246–2254. doi:10.1109/tpwrs.2015.2449667

Liang, R.-H., and Liao, J.-H. (2007). A fuzzy-optimization approach for generation scheduling with wind and solar energy systems. *IEEE Trans. PWRS* 22 (No. 4), 1665–1674. doi:10.1109/tpwrs.2007.907527

Liu, F., Bie, Z., Liu, S., and Ding, T. (2017). Day-ahead optimal dispatch for wind integrated power system considering zonal reserve requirements. *Appl. Energy* 188, 399–408. doi:10.1016/j.apenergy.2016.11.102

Liu, Y., and Nair, N. K. C. (2016). A two-stage stochastic dynamic economic dispatch model considering wind uncertainty. *IEEE Trans. Sustain. Energy* 7 (2), 819–829. doi:10.1109/tste.2015.2498614

Mehdizadeh, A., and Taghizadegan, N. (2017). Robust optimisation approach for bidding strategy of renewable generation-based microgrid under demand side management. *IET Renew. Power Gener.* 11 (11), 1446–1455. doi:10.1049/iet-rpg.2017.0076

Mohammadi-Ivatloo, B., Moradi-Dalvand, M., and Rabiee, A. (2013). Combined heat and power economic dispatch problem solution using particle swarm optimization with time varying acceleration coefficients. *Electr. Power Syst. Res.* 95, 9–18. doi:10.1016/j.epsr.2012.08.005

Mondal, S., Bhattacharya, A., and Nee Dey Halder, S. (2013). Multi-objective economic emission load dispatch solution using gravitational search algorithm and considering wind power penetration. *Electr. Power Energy Syst.* 44 (1), 282–292. doi:10.1016/j.ijepes.2012.06.049

Peng, C., Xie, P., Pan, L., and Yu, R. (2016). Flexible robust optimization dispatch for hybrid wind/photovoltaic/hydro/thermal power system. *IEEE Trans. Smart Grid* 7 (2), 751–762. doi:10.1109/tsg.2015.2471102

Perez-Diaz, J., and Jim, J. (2016). Contribution of a pumped-storage hydropower plant to reduce the scheduling costs of an isolated power system with high wind power penetration. *Energy* 109 (1), 92–104. doi:10.1016/j.energy.2016.04.014

Reddy, S. S., Bijwe, P. R., and Abhyankar, A. R. (2015). Real-time economic dispatch considering renewable power generation variability and uncertainty over scheduling period. *IEEE Syst. J.* 9 (4), 1440–1451. doi:10.1109/jsyst.2014.2325967

Rooijers, F. J., and van Amerongen, R. A. M. (1994). Static economic dispatch for co-generation systems. *IEEE Trans. Power Syst.* 9 (3), 1392–1398. doi:10.1109/59.336125

Shilaja, C., and Ravi, K. (2017). Optimization of emission/economic dispatch using Euclidean affine flower pollination algorithm (eFPA) and binary FPA (BFPA) in solar photo voltaic generation. *Renew. Energy* 107, 550–566. doi:10.1016/j.renene.2017.02.021

Srinivas, N., and Deb, K. (1994). Muiltiobjective optimization using nondominated sorting in genetic algorithms. *IEEE Trans. Evol. Comput.* 2 (3), 221–248. doi:10.1162/evco.1994.2.3.221

Su, C. T., and Chiang, C. L. (2004). An incorporated algorithm for combined heat and power economic dispatch. *Electr. Power Syst. Res.* 69 (2-3), 187–195. doi:10.1016/j.epsr.2003.08.006

Subbaraj, P., Rengaraj, R., and Salivahanan, S. (2009). Enhancement of combined heat and power economic dispatch using self adaptive real-coded genetic algorithm. *Appl. Energy* 86, 915–921. doi:10.1016/j.apenergy.2008.10.002

Tang, Y., Zhong, J., and Liu, J. (2015). A generation adjustment methodology considering fluctuations of loads and renewable energy sources. *IEEE Trans. Power Syst.* 99 (1), 1–8.

Trefny, F. J., and Lee, K. Y. (1981). Economic fuel dispatch. *IEEE Trans. Power Apparatus Syst.* 7, 3468–3477. PAS-100. doi:10.1109/tpas.1981.316690

Vasebi, A., Fesanghary, M., and Bathaee, S. M. T. (2007). Combined heat and power economic dispatch by harmony search algorithm. *Int. J. Electr. Power Energy Syst.* 29 (29), 713–719. doi:10.1016/j.ijepes.2007.06.006

Vemuri, S., Kumar, A. B. R., Hackett, D. F., Eisenhauer, J. T., and Lugtu, R. (1984). Fuel resource scheduling, Part-I- overview of an energy management problem. *IEEE Trans. Power Apparatus Syst.* 7, 1542–1548. PAS-103. doi:10.1109/tpas.1984.318623

Walters, D. C., and Sheble, G. B. (1993). Genetic algorithm solution of economic dispatch with valve point loading. *IEEE Trans. Power Syst.* 8 (3), 1325–1332. doi:10.1109/59.260861

Wang, L., and Singh, C. (2008). Stochastic combined heat and power dispatch based on multi-objective particle swarm optimization. *Int. J. Electr. Power Energy Syst.* 30 (30), 226–234. doi:10.1016/j.ijepes.2007.08.002

Wood, A. J., and Wollenberg, B. F. (1984). *Power generation, operation and control*. New York, NY, USA: Wiley, 230–239.

Yang, L., He, M., Vittal, V., and Zhang, J. (2016). Stochastic optimization-based economic dispatch and interruptible load management with increased wind penetration. *IEEE Trans. Smart Grid* 7 (2), 730–739. doi:10.1109/tsg.2015.2444813

Yousefi, A., Iu, H., Fernando, T., and Trinh, H. (2013). An approach for wind power integration using demand side resources. *IEEE Trans. Sustain. Energy* 4 (4), 917–924. doi:10.1109/tste.2013.2256474

Zitzler, E., Laumanns, M., and Thiele, L. (2001). *SPEA2: improving the strength pareto evolutionary algorithm*. TIK- Report 103. Zurich, Switzerland: Swiss Federal Institute of Technology ETH.

Nomenclature

F_C	Total price function
$f_{sit}(P_{sit})$	Price function of the ith thermal generator at time t
$f_{cit}(P_{cit}, H_{cit})$	Price function of the ith co-generation unit at time t
$f_{hit}(H_{hit})$	Price function of the ith heat-only unit at time t
$a_{si}, b_{si}, c_{si}, d_{si}, e_{si}$	Price coefficients of the ith thermal unit
$\mu_{si}, \kappa_{si}, \pi_{si}, \sigma_{si}, \theta_{si}$	Emission coefficients of the ith thermal unit
$\eta_{si}, \delta_{si}, \mu_{si}, \lambda_{si}, \rho_{si}$	Fuel utilization coefficients of the ith thermal generator
Fst_{im}	Delivered fuel to the ith steam turbine generator in interval m
$Fst_i^{\min}, Fst_i^{\max}$	Lower and upper limits of the fuel delivery of the ith thermal generator
Fsc_{im}	Fuel delivered to the ith co-generation unit in interval m
$Fsc_i^{\min}, Fsc_i^{\max}$	Lower and upper limits of fuel delivery of the ith co-generation unit
F_{Dm}	Total fuel delivered in interval m
P_{sit}	Power output of the ith thermal generating unit at hour t
$P_{si}^{\min}$, $P_{si}^{\max}$	Lower and upper generation limits of the ith thermal generator
UR_i, DR_i	Ramp-up and ramp-down rate limits of the ith thermal generator
P_{cit}, H_{cit}	Power and heat generation of the ith co-generation unit at time t
H_{hit}	Heat generation of the ith heat-only unit at time t
$H_{hi}^{\min}$, $H_{hi}^{\max}$	Lower and upper heat limits of generation of the ith heat-only unit
UR_{ci}, DR_{ci}	Ramp-up and ramp-down rate limits of the ith co-generation unit
$\alpha_{ci}, \beta_{ci}, \gamma_{ci}, \delta_{ci}, \varepsilon_{ci}, \xi_{ci}$	Price coefficients of the ith co-generation unit
τ_{ci}	Emission coefficient of the ith co-generation unit
$\alpha_{si}, \beta_{si}, \gamma_{si}, \delta_{si}, \varepsilon_{si}, \xi_{si}$	Fuel utilization coefficients of the ith co-generation unit
$\phi_{hi}, \psi_{hi}, \chi_{hi}$	Price coefficients of the ith heat-only unit
υ_{hi}	Emission coefficient of the ith heat-only unit
P_{wit}	Obtainable power of the ith wind turbine generator (WTG) at hour t
$P_{wi}^{\min}$, $P_{wi}^{\max}$	Lower and upper limits of generation for ith WTG
P_{wri}	Rated power of ith WTG
Kd_{wi}	Direct price coefficient of ith WTG
ue_{wi}, oe_{wi}	Penalty price and reserve price of ith WTG
$vc_{in} vc_{out}$, vw_r and vw_t	Cut-in, cut-out, rated, and predicted wind pace at time t
P_{PVit}	Output power from the ith solar PV plant at hour t
P_{PVri}	Rated output power of the ith solar PV plant
G_r	Predicted solar irradiation
T_{ref}, T_{ambt}	Reference and ambient temperature
α_r	Coefficient of temperature
Kd_{si}	Direct price coefficient of the ith solar PV plant
ue_{PVi}, oe_{PVi}	Penalty price and reserve price of the ith solar PV plant
Ps_{ghit}	Power generation of the ith pumped hydro storage (PHS) plant at hour t
Ps_{phit}	Pumping power of the ith PHS plant at hour t
$Ps_{ghi}^{\min}$, $Ps_{ghi}^{\max}$	Lower and upper power generation limits of the ith PHS plant

$Ps_{phi}^{\min}$, $Ps_{phi}^{\max}$	Lower and upper pumping power limits of the *i*th PHS plant
Q_{ghit} (Ps_{ghit}) **and** Q_{phit} (Ps_{phit})	Discharge and pumping rate of the *i*th PHS plant at hour *t*
$V_{res,it}$	Volume of water in the upper reservoir of the *i*th PHS plant at hour *t*
$V_{res,i}^{\min}$, $V_{res,i}^{\max}$	Minimum and maximum upper reservoir water storage limits of the *i*th PHS plant
$V_{res,i}^{start}$, $V_{res,i}^{end}$	Specified initial and ending stored water volumes in the upper reservoir of the *i*th PHS plant
Vst_{im}	Fuel storage of the *i*th thermal generator in interval *m*
$Vst_i^{\min}$, $Vst_i^{\max}$	Minimum and maximum fuel storage limits of the *i*th thermal generator
Vst_i^0	Starting fuel storage of the *i*th thermal generator
Vsc_{im}	Fuel storage of the *i*th co-generation unit in intermission *m*
$Vsc_i^{\min}$, $Vsc_i^{\max}$	Lower and upper fuel storage limits of the *i*th co-generation unit
Vsc_i^0	Initial fuel storage of the *i*th co-generation unit
$Incl^{\max}$	Highest augmented load at any hour (MW)
$LF_{Base,t}$	Predicted base power demand at hour *t*
DR_t	Percentage of predicted based power demand partaken in DRP at hour *t*
$Incl_t$	Total augmented power demand at hour *t*
Ls_t	Movable power demand at hour *t*
t, T	Time index and the scheduling period
T_{gen}	Set of all time intermissions when the PHS plant runs as the generation type
T_{pump}	Set of all time intermissions when the PHS plant runs as the pumping type
T_{change_over}	Set of all time intermissions when the PHS plant runs as the idle type
t_m	Duration of the subinterval *m*
M	Number of subintervals
N_c, N_h, N_s , N_w, N_{PV} **and** N_{Pump}	Number of co-generation, heat-only, thermal, TTG, solar PV, and PHS units, respectively